**Title**
Direct observation of permafrost degradation and rapid soil carbon loss in tundra



**Journal**
Nature Geoscience, 12(8)

**ISSN**
1752-0894

**Authors**
Plaza, César
Pegoraro, Elaine
Bracho, Rosvel
et al.

**Publication Date**
2019-08-01

**DOI**
10.1038/s41561-019-0387-6

Peer reviewed

nature geoscience

ARTICLES

https://doi.org/10.1038/s41561-019-0387-6

# Direct observation of permafrost degradation and rapid soil carbon loss in tundra

César Plaza[1,2,3], Elaine Pegoraro[1], Rosvel Bracho[4,7], Gerardo Celis[1], Kathryn G. Crummer[4,7], Jack A. Hutchings[5,8], Caitlin E. Hicks Pries[4,9], Marguerite Mauritz[1], Susan M. Natali[4,10], Verity G. Salmon[4,11], Christina Schädel[1], Elizabeth E. Webb[4] and Edward A. G. Schuur[1,6*]

**Evidence suggests that 5–15% of the vast pool of soil carbon stored in northern permafrost ecosystems could be emitted as greenhouse gases by 2100 under the current path of global warming. However, direct measurements of changes in soil carbon remain scarce, largely because ground subsidence that occurs as the permafrost soils begin to thaw confounds the traditional quantification of carbon pools based on fixed depths or soil horizons. This issue is overcome when carbon is quantified in relation to a fixed ash content, which uses the relatively stable mineral component of soil as a metric for pool comparisons through time. We applied this approach to directly measure soil carbon pool changes over five years in experimentally warmed and ambient tundra ecosystems at a site in Alaska where permafrost is degrading due to climate change. We show a loss of soil carbon of 5.4% per year (95% confidence interval: 1.0, 9.5) across the site. Our results point to lateral hydrological export as a potential pathway for these surprisingly large losses. This research highlights the potential to make repeat soil carbon pool measurements at sentinel sites across the permafrost region, as this feedback to climate change may be occurring faster than previously thought.**

The northern permafrost zone soils cover only 15% of Earth's total soil area but store more than 30% of the global surface soil carbon (C) in the form of organic matter[1,2]. With human-induced warming and permafrost thaw, this vast reserve of permafrost C previously stabilized by low temperatures becomes vulnerable to microbial decomposition, which may further reinforce climate change by releasing significant amounts of carbon dioxide ($CO_2$) and methane ($CH_4$) into the atmosphere[1,3,4].

Despite being the ultimate driver of the permafrost C climate feedback, only a few studies show direct measurements of changing permafrost soil C pools in response to warming[5,6] or warming-affected environmental factors, such as increased nutrient availability[7]. The methods of direct quantification used in previous permafrost studies are similar to those traditionally applied for other soils. Soil samples were collected to a given depth and separated into depth increments of ~5–15 cm. Individual depth increments were then analysed for bulk density and C concentration, from which the C pool, or C mass per unit of surface area, was calculated by summing across depth intervals to a fixed depth or diagnostic horizon (horizontal layers with well-defined characteristics)[5–7]. Permafrost soils typically include organic and mineral diagnostic horizons in a surface active layer that thaws in the summer and refreezes in winter, and overlays perennially frozen horizons[3,6,7]. To quantify changes in permafrost soil C through time based on fixed depths rests on the assumption that the soil bulk density does not also change through time. In the same way, to quantify changes using diagnostic horizons is only possible when the differentiation between horizons is clear and remains constant over time. These conditions, however, are rarely met in thawing permafrost soils. Ice inclusions occur frequently in sizes and shapes that vary from small crystals and lenses (centimetres) to massive wedges (metres) that occupy >50% of the ground volume[3,8]. As permafrost thaws, the thickness of the active layer increases and surface soil collapses into space previously occupied by ice, which results in ground subsidence, soil compaction, increased bulk density and disrupted soil horizons[9].

## Permafrost ecosystem warming experiment

In this study, we directly measured C pool dynamics in a permafrost ecosystem in response to warming by using an equivalent ash mass method to overcome the quantification issues typical of these systems (Supplementary Fig. 1)[10,11]. This method is based on the fact that the mineral component of soil, rather than the depth or horizon differentiation, is not affected by time and treatment (that is, mineral mass is largely conserved). We sampled ambient (control) and experimentally warmed soils ($n=6$ for each treatment) periodically over five years, in 2009, 2010, 2011 and 2013, from the CiPEHR (Carbon in Permafrost Experimental Heating Research) project, a unique ecosystem warming experiment established in 2008 in a moist acidic tundra ecosystem located within the watershed of Eight Mile Lake near Denali National Park, Alaska[12]. The soil in this site comprises an organic horizon approximately 35 cm thick, with C concentrations greater than 20% (Supplementary Fig. 2). The organic horizon overlays the mineral soil of glacial till and windblown loess, with dominant amounts of quartz and

[1]Center for Ecosystem Science and Society, Northern Arizona University, Flagstaff, AZ, USA. [2]Departamento de Biología y Geología, Física y Química Inorgánica, Escuela Superior de Ciencias Experimentales y Tecnología, Universidad Rey Juan Carlos, Móstoles, Spain. [3]Instituto de Ciencias Agrarias, Consejo Superior de Investigaciones Científicas, Madrid, Spain. [4]Department of Biology, University of Florida, Gainesville, FL, USA. [5]Department of Geology, University of Florida, Gainesville, FL, USA. [6]Department of Biological Sciences, Northern Arizona University, Flagstaff, AZ, USA. [7]Present address: School of Forest Resources and Conservation, University of Florida, Gainesville, FL, USA. [8]Present address: Department of Earth and Planetary Sciences, Washington University, St. Louis, MO, USA. [9]Present address: Department of Biological Sciences, Dartmouth College, Hanover, NH, USA. [10]Present address: Woods Hole Research Center, Falmouth, MA, USA. [11]Present address: Environmental Sciences Division, Climate Change Science Institute, Oak Ridge National Laboratory, Oak Ridge, TN, USA. *e-mail: ted.schuur@nau.edu

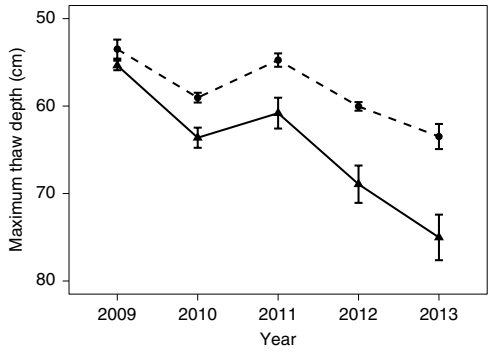


**Fig. 1 | Annual maximum thaw depth (active layer) of permafrost soils in response to ambient (control) and experimental warming.** Circles and dashed lines, ambient; triangles and solid lines, experimental warming (mean ± s.e., $n = 6$ for each group).

feldspars (Supplementary Fig. 3)[13]. We determined the depth profiles of soil mineral concentration (Supplementary Fig. 4) by weighing the ash that remained after laboratory combustion and then calculated the soil C pools on an equivalent ash mass basis. We used cumulative ash pools that approximated 15, 35 and 55 cm depths in the soil cores collected in 2009 (the actual depth per layer and per core was fixed by ash weight, not by distance). We refer to the layers between these limits as surface organic, deep organic and mineral based on the C concentration definition.

Previous work shows the ongoing degradation of the permafrost in our study area in response to changes in the regional climate over the past decades[13–15]. As a result of both the ongoing change in the area and our warming treatment, mean annual temperatures of both ambient and experimentally warmed soils measured at 5, 10, 20 and 40 cm depths increased over time at an average rate that ranged from 0.22 °C yr$^{-1}$ (95% confidence interval (CI): 0.15, 0.29) at 40 cm to 0.28 °C yr$^{-1}$ (95% CI: 0.18, 0.38) at 5 cm (Supplementary Table 1). Compared to ambient, the experimental warming raised the annual average temperatures of the entire soil profile by 0.85–1.01 °C over the five years of study (Supplementary Table 1 and Supplementary Fig. 5).

Consistent with the temperature data, the annual maximum thaw depth (active layer) in ambient soils increased with time at a rate of 2.1 cm yr$^{-1}$ (95% CI: 1.4, 2.9), and the experimental warming significantly accelerated this trend by an additional 2.4 cm yr$^{-1}$ (95% CI: 1.2, 3.5 (Fig. 1 and Supplementary Table 1)). By 2013, the active layer was on average more than 35% deeper in the warming treatment compared to 2009 due to surface permafrost degradation. Ground subsidence, soil compaction and increased waterlogging were visible effects of the deeper thaw on the ambient and especially on the experimentally manipulated plots (Supplementary Fig. 6). We also found that the soil bulk density increased with time, and experimental warming accelerated this effect ($P = 0.036$ (Supplementary Fig. 7 and Supplementary Table 2)).

## C pool changes

Based on the equivalent ash mass, the total soil C pool significantly declined with time at an average rate of 5.4% per year (95% CI: 1.0, 9.5) in response to both ambient and experimental warming (Fig. 2a and Supplementary Tables 3 and 4). The soil N pool also tended to decline at an average rate of 4.3% per year (95% CI: −1.0, 9.1 (Fig. 2b and Supplementary Tables 3 and 4)). After five years, the ambient and experimentally warmed soils lost a total of 6.197 kg m$^{-2}$ of C (95% CI: 1.245, 11.150) and 0.198 kg m$^{-2}$ of N (95% CI: −0.016, 0.412) from the surface, ~0.5 m of soil, which represent 25% (95% CI: 5, 45) and 20% (95% CI: −2, 42) of the initial soil C and N pool at the beginning of the experiment. About 80% of the observed net C losses and 90% of the N losses during the course of the experiment occurred from the mineral horizon (between ~35 and 55 cm) (Fig. 2a,b). The C to N ratio declined markedly with depth and tended to decrease slightly over time (Fig. 2c and Supplementary Tables 3 and 4). C and N losses can be explained as the consequence of soil warming, which in turn results in a deeper thaw, a longer thaw season and higher temperatures throughout the entire active layer. Even though changes in the soil C and N pools were more evident in the experimentally warmed soils and the mean pools were lower, we found no significant differences between the warming and ambient (control) plots ($P > 0.100$ (Fig. 2 and Supplementary Table 4)). This indicates that the effects of the ongoing warming and degradation of the permafrost in our study area were more pronounced than the effects of our experimental manipulation. As well, it may indicate that the deeper soil C exposed in the warming treatments was not equally sensitive to warming and thaw, potentially as a result of decreasing soil C lability with depth.

In northeast Greenland, repeated direct field measurements of soil C to a fixed depth (1 m) did not reveal detectable changes from the thawing permafrost over 12 years, even though warming the same soil in laboratory incubations recorded C loss[5]. Similarly, a previous experiment in Alaska did not find significant changes in the total surface soil C pool after two decades, measured to a common depth (32 cm) in warming and control[6]. Direct measurements of the total soil C pool at our site, if calculated using a fixed depth of 55 cm, averaged 39.5 kg m$^{-2}$ (95% CI: 34.3, 44.8) in 2009 and 40.2 kg m$^{-2}$ (95% CI: 33.9, 46.5) in 2013, and also did not detect the change over time. Using a fixed depth fails to detect the significant change in soil C that is revealed when correcting for ground subsidence and soil compaction, because additional C that was once deeper becomes included in the fixed-depth inventory and masks losses from the original pool.

Recent chronosequence and modelling results also indicated rapid C loss from boreal peatlands (~30% of the initial C stock over a decade) after permafrost thaw[16]. From the perspective of climate change, C loss from permafrost soils may be counterbalanced by increased plant C uptake and growth due to the stimulating effect of higher temperatures and atmospheric $CO_2$ levels, longer growing seasons and the augmented availability of nutrients[17]. Previous work at the CiPEHR site showed that the above-ground plant biomass was about 0.400 kg m$^{-2}$ and increased by approximately 0.150 kg m$^{-2}$ in our ambient plots and by 0.300 kg m$^{-2}$ in the experimental warming plots from 2009 to 2013. The increase in plant growth was attributed to increases in nutrients as additional N was released from the active layer[18]. Assuming that the C concentration is 50% of the plant tissue, we estimated that increases in above-ground plant biomass C offset less than 2.5% of the mean soil C pool loss during the same period. The relatively small net C loss measured in the organic layer does suggest offsets by fresh plant material that enters the soil surface. In contrast, below-ground C inputs derived from roots did not offset the much larger net C loss in the mineral layer. The C concentration of the mineral soil layer (~19% C) was very large compared to that generally found in temperate mineral soils. This and the typically low reactivity of minerals in Arctic soils[3] suggest that much of the original C in this deeper layer was climatically stabilized and protected from microbial decomposition due to the low temperatures and not primarily because of the association with mineral surfaces and soil aggregates, which are major mechanisms that limit the decomposition of C in mineral soils elsewhere[19,20].

## Pathways of C loss

The net C loss as a result of soil warming, permafrost thaw and increased microbial activity is expected to alter the remaining soil organic matter due to the differential consumption of C compounds during decomposition. We tested this hypothesis using NMR spectroscopy to examine changes in the molecular imprint of the

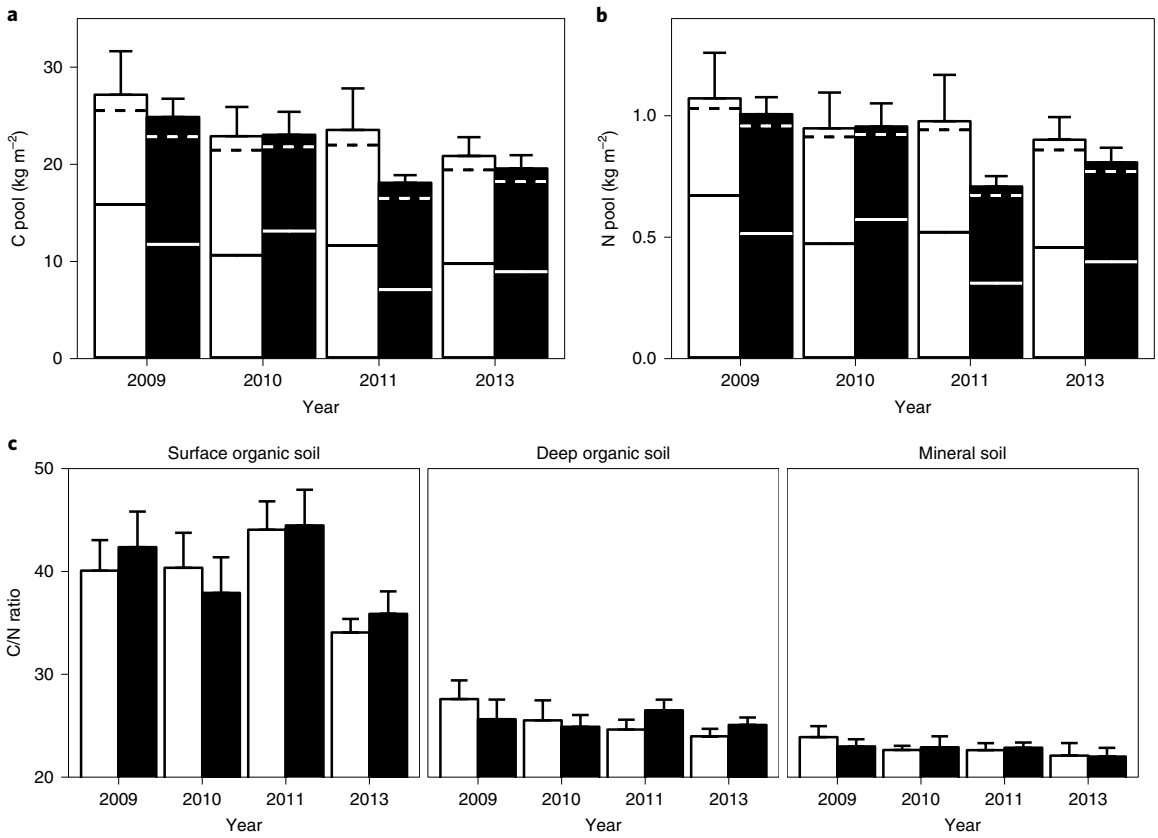


**Fig. 2 | Pools of ambient (control) and warmed permafrost soils. a–c**, The pools of C (**a**) and N (**b**) and the ratio of C to N (**c**) were calculated on equivalent ash masses that corresponded to approximately 15, 35 and 55 cm in depth in 2009. Continuous lines within the bars separate the organic (top, ~0–35 cm) from the mineral (bottom, ~35–55 cm) layer pools; dashed lines separate the surface (~0–15 cm) organic (top) from the deep (~15–35 cm) organic (bottom) pools. White bars, ambient warming; black bars, experimental warming (mean + s.e., $n = 6$, except for the warmed mineral layer in 2011, for which $n = 5$).

organic matter over time with the experimental warming. During decomposition, large plant constituents of soil organic matter, rich in structural carbohydrates, are continuously processed to smaller fragments and molecules with concomitant $CO_2$ emissions and enrichment in microbial by-products[20,21]. The NMR spectra of all the soils (Supplementary Fig. 8) were dominated by signals in the *O*-alkyl C region attributable to carbohydrates primarily from relatively unaltered large plant fragments, and in the unsubstituted alkyl C region most probably arise from the lipids and peptides from plant- and microbial-derived materials[21]. From 2009 to 2013, the intensity of the carbohydrate signals in the *O*-alkyl C region relative to those in the unsubstituted alkyl C region declined in the surface organic layer in both the ambient and the experimental warming plots (Fig. 3). The decline was consistent with increased organic matter decomposition and in situ C gas emission that prevailed over the increased plant C inputs in this upper layer. In striking contrast, the carbohydrate signals in the *O*-alkyl C region relative to those in the unsubstituted alkyl C region remained unchanged in the deep organic layer and actually increased in the mineral layer (Fig. 3), in which the majority of the C loss occurred. The addition of some organic materials richer in carbohydrates from the layers above or new C as a result of plant roots growing deeper could have left an imprint on the *O*-alkyl C region. However, the apparent increase in the *O*-alkyl C region in a horizon that loses net C implies the preferential loss of more decomposed materials. The preferential loss of more decomposed C might occur if smaller molecules were more prone than larger plant-derived macromolecules to removal in water as lateral C export[20], or if the decomposition of more-processed C was more sensitive to changes in temperature that occurred as a result of warming[22].

On warming, soil C loss may occur through the emissions of $CO_2$ and $CH_4$ and hydrological transport of particulate and dissolved C as organic matter is transformed by the soil decomposer community. In situ decomposition and ecosystem–atmosphere $CO_2$ exchange from our plots was quantified in previous chamber and flux tower studies, but cannot fully explain the magnitude of the total soil pool C loss observed with the direct measurements presented here[12,23]. In particular, depending on the method used to measure non-growing season (October–April) fluxes, the estimated annual net C loss via $CO_2$ emission ranged from 0.027 to 0.130 $kg\,m^{-2}\,yr^{-1}$ for the ambient soil and from 0.022 to 0.123 $kg\,m^{-2}\,yr^{-1}$ for the experimentally warmed soil[12,23]. Also, although annual estimates of the $CH_4$ flux at this site have not yet been made, the much smaller total C loss expected as a result of anaerobic processes[24] and supported by previous field studies in other Arctic and boreal systems[25] show that the expected losses might be on the order of tens of grams of $CH_4$-C $m^{-2}\,yr^{-1}$ at most. Together, the net exchange of $CO_2$ and $CH_4$ gases appears to account for much less than 50% of the observed soil C loss.

These results then point to the lateral hydrological export of C as a potential pathway for significant soil C loss from the site, which potentially accounts for more than half of the observed decline. Vertical drainage is impeded by the permafrost surface and lateral flow through the soil profile carries dissolved inorganic C produced

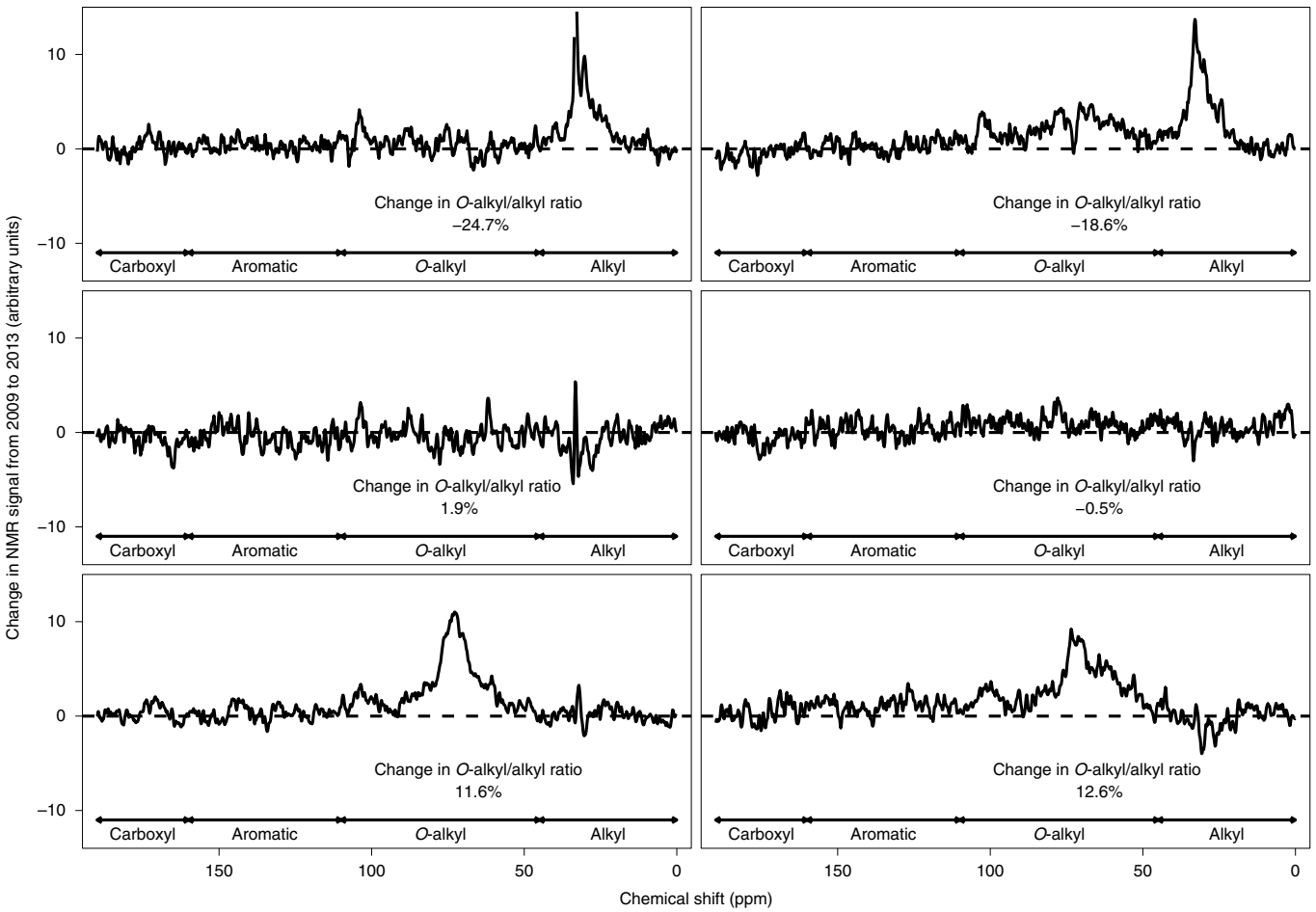


**Fig. 3 | Changes in $^{13}C$ NMR spectra of ambient (control (left)) and experimentally warmed (right) permafrost soils after five years of treatment.** The NMR signals of the surface organic (top), deep organic (middle) and mineral (bottom) layers in 2013 after subtracting the spectra of the corresponding soils in 2009. *O*-alkyl to alkyl ratios, which typically decrease with progressive decomposition, were calculated by dividing the area under the signal of the *O*-alkyl region (45–95 ppm) by the area under the signal of the alkyl region (0–45 ppm).

by respiration, as well as dissolved and particulate organic C, away from the ecosystem into rivulets and small streams[26]. Once it enters the aquatic environment, C can either be emitted to the atmosphere, or undergo further transformations—the fate of the transported C is highly uncertain. These fluxes have also been shown to typically be on the order of tens of grams of C per square metre per year each for dissolved organic, inorganic and particulate C across a range of Alaskan watersheds[27]. Of the three lateral export forms, particulate C is the only one observed in some degrading permafrost landscapes to attain the magnitude of hundreds of grams of C per square metre per year necessary to explain our observed C stock change[28], albeit the potential for similarly high losses of dissolved organic C from our soils has been shown in laboratory column experiments[29].

## Implications

If the C losses quantified here follow the exponential nature of soil C dynamics, they are likely to continue but would be expected to attenuate over time. A simple calculation (Supplementary Methods) based on the initial measured rates of plant C input ranging from 0.1 to 0.3 kg $m^{-2}$ $yr^{-1}$ and increasing by 1% $yr^{-1}$ can be made to allow for future increases in plant growth and new soil C inputs. New inputs, offset by exponential outputs of current soil C at rates estimated by our direct measurements, translate into a net loss of 16–17 kg C $m^{-2}$ by 2030 and 17–21 kg C $m^{-2}$ by 2100, approximately 61–64% and 6–78% of the original 27 kg C $m^{-2}$ in the top ~55 cm of soil, of which up to three-quarters of the total projected loss occurs in the mineral layer. This estimate of the net C loss is consistent with a lower soil C storage in high-latitude non-permafrost soils[30].

The latest expert assessments based on laboratory incubations, gas flux measurements and modelling suggest that 5–15% of the permafrost soil C could be released to the atmosphere by the end of this century under the current global warming scenario[1]. The simple modelling exercise presented here agrees with the observations that our study site was crossing a phase of rapid change at the time of the experiment, and also demonstrates the potential significant loss of soil C as a result of permafrost thaw, which exceeds the current projections of soil C loss and $CO_2$ emissions for the Eight Mile Lake watershed, Arctic tundra, and the entire permafrost region[1,13,31]. Our results demonstrate the potential for repeated measurements that quantify changes in soil C across the entire permafrost region to better understand its environmental fate. An effort such as this is a critical and currently overlooked link to determine the magnitude of the terrestrial permafrost C feedback to climate change.

## Online content

Any methods, additional references, Nature Research reporting summaries, source data, statements of code and data availability and associated accession codes are available at https://doi.org/10.1038/s41561-019-0387-6.

Received: 30 October 2018; Accepted: 13 May 2019;
Published online: 1 July 2019

## References


1. Schuur, E. A. G. et al. Climate change and the permafrost carbon feedback. *Nature* **520**, 171–179 (2015).
2. Hugelius, G. et al. Estimated stocks of circumpolar permafrost carbon with quantified uncertainty ranges and identified data gaps. *Biogeosciences* **11**, 6573–6593 (2014).
3. Ping, C. L., Jastrow, J. D., Jorgenson, M. T., Michaelson, G. J. & Shur, Y. L. Permafrost soils and carbon cycling. *Soil* **1**, 147–171 (2015).
4. Schaefer, K., Lantuit, H., Romanovsky, V. E., Schuur, E. A. G. & Witt, R. The impact of the permafrost carbon feedback on global climate. *Environ. Res. Lett.* **9**, 085003 (2014).
5. Elberling, B. et al. Long-term $CO_2$ production following permafrost thaw. *Nat. Clim. Change* **3**, 890–894 (2013).
6. Sistla, S. A. et al. Long-term warming restructures Arctic tundra without changing net soil carbon storage. *Nature* **497**, 615–618 (2013).
7. Mack, M. C., Schuur, E. A. G., Bret-Harte, M. S., Shaver, G. R. & Chapin, F. S. III Ecosystem carbon storage in Arctic tundra reduced by long-term nutrient fertilization. *Nature* **431**, 440–443 (2003).
8. Strauss, J. et al. The deep permafrost carbon pool of the Yedoma region in Siberia and Alaska. *Geophys. Res. Lett.* **40**, 6165–6170 (2013).
9. Jorgenson, M. T. & Osterkamp, T. E. Response of boreal ecosystems to varying modes of permafrost degradation. *Can. J. For. Res.* **35**, 2100–2111 (2005).
10. Grønlund, A., Hauge, A., Hovde, A. & Rasse, D. P. Carbon loss estimates from cultivated peat soils in Norway: a comparison of three methods. *Nutr. Cycl. Agroecosys.* **81**, 157–167 (2008).
11. Rogiers, N., Conen, F., Furger, M., Stöckli, R. & Eugster, W. Impact of past and present land-management on the C-balance of a grassland in the Swiss Alps. *Glob. Change Biol.* **14**, 2613–2625 (2008).
12. Natali, S. M., Schuur, E. A. G., Webb, E. E., Hicks Pries, C. E. & Crummer, K. G. Permafrost degradation stimulates carbon loss from experimentally warmed tundra. *Ecology* **95**, 602–608 (2014).
13. Schuur, E. A. G. et al. The effect of permafrost thaw on old carbon release and net carbon exchange from tundra. *Nature* **459**, 556–559 (2009).
14. Romanovsky, W. E. et al. Permafrost. *Arctic Report Card* http://www.arctic.noaa.gov/reportcard (2012).
15. Osterkamp, T. E. Characteristics of the recent warming of permafrost in Alaska. *J. Geophys. Res.* **112**, F02S02 (2007).
16. Jones, M. C. et al. Rapid carbon loss and slow recovery following permafrost thaw in boreal peatlands. *Glob. Change Biol.* **23**, 1109–1127 (2017).
17. Shaver, G. R. et al. Global warming and terrestrial ecosystems: a conceptual framework for analysis. *Bioscience* **50**, 871–882 (2000).
18. Salmon, V. G. et al. Nitrogen availability increases in a tundra ecosystem during five years of experimental permafrost thaw. *Glob. Change Biol.* **22**, 1927–1941 (2016).
19. Schmidt, M. W. I. et al. Persistence of soil organic matter as an ecosystem property. *Nature* **478**, 49–56 (2011).
20. Lehmann, J. & Kleber, M. The contentious nature of soil organic matter. *Nature* **528**, 60–68 (2015).
21. Baldock, J. A. & Skjemstad, J. O. Role of the soil matrix and minerals in protecting natural organic materials against biological attack. *Org. Geochem.* **31**, 697–710 (2000).
22. Davidson, E. A. & Janssens, I. A. Temperature sensitivity of soil carbon decomposition and feedbacks to climate change. *Nature* **440**, 165–173 (2006).
23. Webb, E. E. et al. Increased wintertime $CO_2$ loss as a result of sustained tundra warming. *J. Geophys. Res. Biogeosci.* **121**, 249–265 (2016).
24. Schädel, C. et al. Potential carbon emissions dominated by carbon dioxide from thawed permafrost soils. *Nat. Clim. Change* **6**, 950–953 (2016).
25. Olefeldt, D., Turetsky, M. R., Crill, P. M. & McGuire, A. D. Environmental and physical controls on northern terrestrial methane emissions across permafrost zones. *Glob. Change Biol.* **19**, 589–603 (2013).
26. Vonk, J. E. & Gustafsson, O. Permafrost–carbon complexities. *Nat. Geosci.* **2**, 598–600 (2013).
27. Zhu, Z. & McGuire, A. D. *Baseline and Projected Future Carbon Storage and Greenhouse-Gas Fluxes in Ecosystems of Alaska* Professional Paper 1826 (USGS, 2016).
28. Abbott, B. W. & Jones, J. B. Permafrost collapse alters soil carbon stocks, respiration, $CH_4$, and $N_2O$ in upland tundra. *Glob. Change Biol.* **21**, 4570–4587 (2015).
29. Zhang, X. et al. Importance of lateral flux and its percolation depth on organic carbon export in Arctic tundra soil: implications from a soil leaching experiment. *J. Geophys. Res.* **122**, 796–810 (2017).
30. Tarnocai, C. et al. Soil organic carbon pools in the northern circumpolar permafrost region. *Glob. Biogeochem. Cycl.* **23**, GB2023 (2009).
31. McGuire, A. D. et al. An assessment of the carbon balance of Arctic tundra: comparisons among observations, process models, and atmospheric inversions. *Biogeosciences* **9**, 3185–3204 (2012).


## Acknowledgements

This work was based in part on support provided by the following programs: US Department of Energy, Office of Biological and Environmental Research, Terrestrial Ecosystem Science (TES) Program, Award nos DE-SC0006982 and DE-SC0014085; National Science Foundation CAREER program, Award no. 0747195; National Parks Inventory and Monitoring Program; National Science Foundation Bonanza Creek LTER program, Award no. 1026415 and National Science Foundation Office of Polar Programs, Award no. 1203777. In addition, this project received funding from the European Union's Horizon 2020 research and innovation programme under the Marie Skłodowska Curie grant agreement 654132. We thank L. Barrios (CSIC) and the NAU statistical consulting lab for assistance with the data analysis.

## Author contributions

E.A.G.S. conceived and designed the study. E.A.G.S. and S.M.N. implemented the field experiment. R.B., G.C., K.G.C., J.A.H., M.M., S.M.N., C.P., C.E.H.P., E.P., C.S., E.A.G.S., V.G.S. and E.E.W. performed the field research and/or data analysis. K.G.C., J.A.H., C.P., E.P., M.M., S.M.N. and V.G.S. conducted the laboratory research. C.P., G.C. and M.M. carried out data analyses. C.P., E.A.G.S. and E.P. wrote the article. All authors substantially discussed the results and contributed to editing the manuscript.

## Competing interests

The authors declare no competing interests.

## Additional information

**Supplementary information** is available for this paper at https://doi.org/10.1038/s41561-019-0387-6.

**Reprints and permissions information** is available at www.nature.com/reprints.

**Correspondence and requests for materials** should be addressed to E.A.G.S.

**Publisher's note:** Springer Nature remains neutral with regard to jurisdictional claims in published maps and institutional affiliations.

## Methods

**Site description.** The experimental site was established within the watershed of Eight Mile Lake in Healy, Alaska (63° 52′ 59″ N, 149° 13′ 32″ W). The climate is subarctic, with air temperatures that remain consistently below 0 °C from mid-October to late March. Monthly averages range from −17 °C in December to 15 °C in July and the annual average is −1.0 °C. The mean annual precipitation is 378 mm, more than half of which falls in June, July and August. The permafrost where the experiment is located is especially sensitive to warming because its annual mean temperature is close to freezing point, only a few tenths below 0 °C (ref. [14]). The vegetation is moist acidic tundra. The vascular plant biomass mainly includes the tussock-forming sedge *Eriophorum vaginatum* and deciduous shrubs *Betula nana* and *Vaccinium uliginosum*, whereas non-vascular cover is dominated by feather moss (primarily *Pleurozium schreberi*) and *Sphagnum* spp., as well as several lichen species (primarily *Cladonia* spp.). The soil is classified as a gelisol[32], composed of an organic horizon (35 cm thick) on top of a cryoturbated mineral horizon that consists of a mixture of glacial till and windblown loess[33,34]. The site is located on a gentle slope, and the active soil layer is relatively well drained[35].

**Experimental design.** The experiment, CiPEHR, was set up in 2008. The experimental warming treatment was applied with six replicate snow fences (1.5 m tall × 8 m long) in three blocks (100 m apart) distributed throughout the landscape. For comparison, a recent meta-analysis of soil warming experiments[36] compiled the results of a large number of existing soil warming experiments (49 in total). Only 20% of all those experiments had a replicate number equal to six or higher, and only 6% of all the experiments had a replicate number higher than six. Fences were installed perpendicular to dominant southeasterly winter winds so that snow was deposited on the leeward side of the fence. Increased snow depth acts as an insulating layer that keeps the soil warmer in the winter and in the summer. Excess snow relative to the ambient (control) treatment was removed in the spring before the snowmelt to ensure the same water inputs into the soil. Soil temperatures at 5, 10, 20 and 40 cm were monitored continuously from October 2008 through September 2013 with copper–constantan thermocouples. The maximum thaw depth was measured annually in mid-September with a 3 mm diameter metal rod inserted vertically into the soil. The water table depth was measured using monitoring wells. Other core measurements in the experimental plots included soil moisture, $CO_2$ fluxes and plant productivity. Further details of the experimental design are reported elsewhere[33,34].

**Soil sampling, preparation and analysis.** Soil samples were collected within the footprint of each fence from control ($n = 6$) and warming ($n = 6$) plots in May or June 2009, 2010, 2011 and 2013. At the sampling times, the entire soil profile was frozen except for a few centimetres below the surface, and no standing water that was unfrozen was visible at the site. We sampled when the soils were still frozen to obtain intact cores and prevent problems of soil compaction. The surface thawed soil was cut out into 10 cm × 10 cm rectangular sections using a serrated knife. The underlying frozen soil was sampled using a permafrost drill with a 7.6 cm diameter hollow carbide bit to the depth at which rocks impeded the coring. In the laboratory, the soil samples were sectioned into 5 cm at the surface and at 10 cm depth increments thereafter, and the sections were weighed[37]. Down to 35–45 cm, the number of core segments were six for each treatment; from 35–45 to 85–95 cm, the number of core segments varied from one to six due to varying core lengths (for the control soil in 2009, $n = 4$ for 55–65 cm, 3 for 65–75 cm and 1 for 75–85 cm; for the experimentally warmed soil in 2009, $n = 5$ for 65–75 cm and 75–85 cm; for the control soil in 2010, $n = 5$ for 55–65 cm and 1 for 65–75 cm; for the experimentally warmed soil in 2010, $n = 5$ for 45–55 cm, 3 for 55–65 and 65–75 cm and 2 for 75–85 cm; for control soil in 2011, $n = 2$ for 55–65 cm; for experimentally warmed soil in 2011, $n = 5$ for 35–45 cm, 2 for 45–55 and 55–65 cm, and 1 for 65–75 cm; for control soil in 2013, $n = 4$ for 75–85 cm; for experimentally warmed soil in 2013, $n = 5$ for 65–75 cm, 3 for 75–85 cm and 1 for 85–95). The moisture (ice) content was determined by mass loss after oven-drying at 60 °C for 3 d (Supplementary Fig. 9). The bulk density was calculated as the dry mass of each depth section divided by its frozen volume. The ash concentration was determined on dried, ground soil subsamples by mass loss after heating at 550 °C for 12 h. C and N concentrations were determined by dry combustion using a Costech Analytical ECS 4010 elemental analyser. We conducted one analysis per sample. We included a standard every ten samples as the quality control, and the relative s.d. was less than 2% for both C and N. The soil mineral composition was examined by X-ray powder diffraction on a composite sample of the mineral layer using a Philips X'Pert diffractometer with Cu Kα radiation and a scan rate of 0.02° $2\theta\,s^{-1}$; speciation was assessed by comparison with the International Center for Diffraction data. Oven-drying is a standard procedure of sample pretreatment for soil organic C analysis, but may cause some systematic error due to the oxidation of labile organic matter[38,39].

**Soil C and N pools.** Soil C and N pools were calculated on an equivalent ash mass basis, similar to previous work using equivalent soil and mineral mass approaches[39–41]. For this purpose, we first calculated the cumulative mass of ash (AM ($kg\,m^{-2}$)) to the deeper end of each core segment:

$$\mathrm{AM}_i = \sum_{i=1}^{n} \left( \frac{A_i \times \mathrm{BD}_i \times L_i}{100} \right)$$

where $A_i$ is the ash concentration ($g\,kg^{-1}$), $\mathrm{BD}_i$ is the bulk density ($g\,cm^{-3}$), and $L_i$ is the length (cm) of the core segment $i$. Similarly, we calculated the cumulative pool of C and N (XP ($kg\,m^{-2}$)) to the deeper end of each core segment:

$$\mathrm{XP}_i = \sum_{i=1}^{n} \left( \frac{X_i \times \mathrm{BD}_i \times L_i}{100} \right)$$

where $X_i$ is the C or N concentration ($g\,kg^{-1}$) of the of the core segment $i$. Finally, we calculated the soil C and N pools to three given equivalent ash masses ($\mathrm{XP}_{\mathrm{EAM}}$ ($kg\,m^{-2}$)) by linear interpolation within the range of data points for the deepest core segment ($d$) required to attain the equivalent ash mass (EAM):

$$\mathrm{XP}_{\mathrm{EAM}} = \mathrm{XP}_{d-1} + (\mathrm{EAM} - \mathrm{AM}_{d-1}) \frac{\mathrm{XP}_d - \mathrm{XP}_{d-1}}{\mathrm{AM}_d - \mathrm{AM}_{d-1}}$$

where $\mathrm{XP}_{d-1}$ is the cumulative pool of C or N ($kg\,m^{-2}$) to the deeper end of the core segment above the core segment required to attain the EAM, $\mathrm{AM}_{d-1}$ is the cumulative ash mass ($kg\,m^{-2}$) to the deeper end of the core segment above the core segment required to attain the EAM, $\mathrm{XP}_d$ is the cumulative pool of C or N ($kg\,m^{-2}$) to the deeper end of the core segment required to attain the EAM and $\mathrm{AM}_d$ is the cumulative ash mass ($kg\,m^{-2}$) to the deeper end of the core segment required to attain the EAM. As the EAMs, we used the smallest cumulative ash masses to depths of 15, 35 and 55 cm in the soil cores collected in 2009, which were 0.4, 6.1 and 49.4 $kg\,m^{-2}$, respectively, and we refer to the layers between those limits as surface organic, deep organic and mineral based on the C concentration definition for those diagnostic horizons. In particular, we used a cutoff organic C concentration of 20% to distinguish mineral from organic soil layers[42]. On this basis, the soil profile in 2009 comprised an organic horizon 35 cm thick, with an average C concentration greater than 20%, that overlaid mineral soil material, with an average C concentration less than 20% (Supplementary Fig. 2). We further distinguished the surface and deep organic layers by separating the depth increments to 35 cm into 0–15 cm and 15–35 cm, to gain an insight into the organic soil horizon. For the C and N pool calculations, we only used data to the depth that corresponded to the smallest cumulative ash pool to a depth of 55 cm in the cores collected in 2009. As the bulk density increased (soil compacted) over time, the depths in 2010, 2011 and 2013 required to attain the EAM mass did not extend below 55 cm. The calculations are illustrated in Supplementary Table 4 with specific data from two sample soil cores collected in 2009 and 2013.

This method assumes that the total mass of ash (primarily soil minerals) is conserved along the soil profile over time (that is, there is no net lateral gain or loss of ash or exogenous ash deposition on the soil surface). Although there is no evidence of change, ash losses from the soil would lead to an underestimation of C and N losses by this method, whereas increases in the ash content from exogenous deposition would lead to an overestimation. Cryoturbation, or freeze–thaw mixing of the soil horizons in the active layer, is a widespread process in permafrost soils that could incorporate organic matter at depth and move subsoil materials relatively richer in ash (minerals) upward[3]. This phenomenon, however, is believed to operate at timescales longer than 5 yr (ref. [43]). Further, we found no evidence of organic matter burial at any depth between the soil layer examined (~0–55 cm) and 85 cm below the active layer (cryoturbation and burial below the active layer is impeded by the permafrost). Previous work used similar equivalent ash mass methods to provide reliable estimates of the C changes in highly organic soils in response to land management[10,11].

**Nuclear magnetic resonance.** For $^{13}C$ cross-polarization with magic angle spinning (CP-MAS) NMR analysis, composite samples of ambient and experimentally surface organic, deep organic and mineral soils in 2009 and 2013 were prepared by mixing the corresponding mass proportions of the depth sections and equal masses of the six core replicates for each treatment. Replicate measurements are very rare in NMR environmental studies because of the high cost and long time required for NMR analysis, and the preparation of composite samples from experimental replicates is a common approach to attain representativeness and reproducibility[44]. The spectra were acquired on a Bruker AV 400 MHz spectrometer equipped with a 4 mm $^1H/X/Y$ MAS probe operated at a MAS frequency of 13,000 Hz, a ramp–CP contact time of 1 ms, a recycle delay of 1 s and 8,192, 16,384, and 57,117 scans for the surface organic, deep organic and mineral soil samples, respectively. The free induction decay signal was digitized and multiplied by an exponential function that corresponded to a 60 Hz line broadening in the final transformed spectrum. The spectra were then baseline corrected, calibrated relative to adamantane and integrated into the following chemical shift regions: 0–45 ppm, alkyl C; 45–95 ppm, *O*-alkyl C; 95–110 ppm, anomeric C; 110–160 ppm, aromatic C and 160–200 ppm, carboxyl and carbonyl C (ref. [45]). Similar to previous NMR environmental studies[44], variations greater than 2.0% in the signal intensity within a given spectral region were deemed significant.

**Statistical analysis.** Linear mixed-effects modelling was used to test for the main and interaction effects of the explanatory variables on the soil response variables investigated. Experimental warming and depth were incorporated as categorical variables and time was included as a continuous covariate after mean centring. To account for the lack of independence in the residuals due to the repeated measures and blocked split-plot design, a slope and intercept structure was first incorporated in the random term of the model, with time as a continuous covariate and block, fence nested in block and warming nested in fence as the categorical variables. The structure of the random model component was then optimized through a backward stepwise procedure, using all the explanatory variables and their interactions in the fixed component and the second-order Akaike information criterion for small sample sizes and likelihood ratio tests for model selection[46]. In particular, the only effects retained were those that, on removal, caused an increase of the Akaike information criterion and a likelihood ratio test with a *P* value (based on Satterthwaite approximation) of less than 0.10 (ref. [47]). Once the optimal random component was found, the fixed effects were determined using a similar top-down model selection strategy. The coefficients of the optimal model were estimated by the restricted maximum likelihood approach, and 90 and 95% bootstrap CIs were calculated based on 1,000 simulations. Uncertainties in the pool changes were calculated using error propagation formula[48]. The validity of the assumptions of normality and homoscedasticity were examined using residual plots. All the statistical analyses and plots were performed using R[49] and the R packages lme4[50], lmerTest[51], MuMIn[52], ggplot2[53] and cowplot[54].

## Data availability

All the data and metadata associated with this manuscript are deposited in the Long Term Ecological Research (LTER) Network Information System Data Portal at https://portal.lternet.edu/nis/home.jsp (https://doi.org/10.6073/pasta/894ec9847bc365347775d3aaba44a50210.6073/pasta/894ec9847bc365347775d3aaba44a502, https://doi.org/10.6073/pasta/f502d8fe1a2e1d6c6b035c198af04f3e and https://doi.org/10.6073/pasta/b559d2650efe99ccabb2a58d9d8819ab).

## References


32. Soil Survey Staff *Keys to Soil Taxonomy* (USDA–NRCS, 2014).
33. Natali, S. et al. Effects of experimental warming of air, soil and permafrost on carbon balance in Alaskan tundra. *Glob. Change Biol.* **17**, 1394–1407 (2011).
34. Natali, S., Schuur, E. & Rubin, R. Increased plant productivity in Alaskan tundra as a result of experimental warming of soil and permafrost. *J. Ecol.* **100**, 488–498 (2012).
35. Mauritz, M. et al. Nonlinear $CO_2$ flux response to 7 years of experimentally induced permafrost thaw. *Glob. Change Biol.* **23**, 3646–3666 (2017).
36. Crowther, T. W. et al. Quantifying global soil carbon losses in response to warming. *Nature* **540**, 104–108 (2016).
37. Hicks Pries, C. E., Schuur, E. A. G. & Crummer, K. G. Holocene carbon stocks and carbon accumulation rates altered in soils undergoing permafrost thaw. *Ecosystems* **15**, 162–173 (2012).
38. Schumacher, B. A. *Methods for the Determination of Total Organic Carbon (TOC) in Soils and Sediments* EPA/600/R-02/069 (US EPA, 2002).
39. Ellert, B. H., Janzen, H. H., VandenBygaart, A. G. & Bremer, E., in *Soil Sampling and Methods of Analysis* (eds Carter, M. R. & Gregorich, E. G.) 25–38 (CRC Press, 2007).
40. Lee, J., Hopmans, J. W., Rolston, D. E., Baer, S. G. & Six, J. Determining soil carbon stock changes: simple bulk density corrections fail. *Agric. Ecosyst. Environ.* **134**, 251–256 (2009).
41. McBratney, A. B. & Minasny, B. Comment on "Determining soil carbon stock changes: simple bulk density corrections fail". *Agric. Ecosyst. Environ.* **136**, 185–186 (2010).
42. IUSS Working Group WRB *World Reference Base for Soil Resources 2014* (FAO, 2014).
43. Kaiser, C. et al. Conservation of soil organic matter through cryoturbation in Arctic soils in Siberia. *J. Geophys. Res.* **112**, G02017 (2007).
44. Baldock, J. A. & Smernik, R. J. Chemical composition and bioavailability of thermally altered *Pinus resinosa* (Red pine) wood. *Org. Geochem.* **33**, 1093–1109 (2002).
45. Simpson, A. J. & Simpson, M. J. in *Biophysico-Chemical Processes Involving Natural Nonliving Organic Matter in Environmental* Systems (eds Senesi, N., Xing, B. & Huang, P. M.) 589–651 (John Wiley & Sons, 2009).
46. Zuur, A. F., Ieno, E. N., Walker, N. J., Saveliev, A. A. & Smith, G. M. *Mixed Effects Models and Extensions in Ecology with R* (Springer, 2009).
47. Burnham, K. P. & Anderson, D. R. *Model Selection and Multimodel Inference: A Practical Information-Theoretic Approach* (Springer, 2002).
48. Ku, H. H. Notes on the use of propagation of error formulas. *J. Res. Natl Bur. Stand. C* **70C**, 263–273 (1966).
49. R Core Team. *R: A language and environment for statistical computing* https://d.R-project.org (2015).
50. Bates, D., Mächler, M., Bolker, B. & Walker, S. Fitting linear mixed-effects models using lme4. *J. Stat. Softw.* **67**, 1–48 (2015).
51. Kuznetsova, A., Brockhoff, P. B. & Christensen, R. H. B. *lmerTest: Tests in Linear Mixed Effects Models* https://CRAN.R-project.org/package=lmerTest (2016).
52. Barton, K. *MuMIn: Multi-Model inference* https://CRAN.R-project.org/package=MuMIn (2016).
53. Wickham, H. *ggplot2: Elegant Graphics for Data Analysis* (Springer, 2009).
54. Wilke, C. O. cowplot: Streamlined Plot Theme and Plot Annotations for 'ggplot2' https://CRAN.R-project.org/package=cowplot (2016).